

Threading-Induced Dynamical Transition in Chimeric Polymers

A. Rosa,^{1,*} J. Smrek,^{2,*} M. S. Turner,^{3,4} and D. Michieletto^{5,6,7,†}

¹*Sissa (Scuola Internazionale Superiore di Studi Avanzati), Via Bonomea 265, 34136 Trieste, Italy*

²*Faculty of Physics, University of Vienna, Boltzmanngasse 5, A-1090 Vienna, Austria*

³*Department of Physics and Centre for Complexity Science,
University of Warwick, Coventry, CV4 7AL, UK*

⁴*Department of Chemical Engineering, Kyoto University, Kyoto, Japan*

⁵*School of Physics and Astronomy, University of Edinburgh,
Peter Guthrie Tait Road, Edinburgh, EH9 3FD, UK*

⁶*MRC Human Genetics Unit, Institute of Genetics and Molecular Medicine,
University of Edinburgh, Edinburgh EH4 2XU, UK*

⁷*Department of Mathematical Sciences, University of Bath, North Rd, Bath BA2 7AY, UK*

The relationship between polymer topology and bulk rheology remains a key question in soft matter physics. Architecture-specific constraints (or threadings) are thought to control the dynamics of circular polymers in ring-linear blends where the dynamics are enslaved by the reptative motion of the linear fraction. Here we consider qualitatively different systems of linear and circular polymers, fused together in “chimeric” architectures. The simplest example of this family is a “tadpole”-shaped polymer – a single ring fused to the end of a single linear chain. We show that polymers with this architecture display a threading-induced dynamical transition that substantially slows chain relaxation. Our findings shed light on how threadings control dynamics and may inform design principles for chimeric polymers with topologically-tunable bulk rheological properties.

The tube and reptation theories underpin our understanding of complex fluids [1, 2]. However, the seemingly innocuous joining of the polymers’ ends to form rings poses a problem that has been puzzling the polymer physics community for over three decades [3–20].

Entangled solutions of extremely pure unlinked ring polymers [11, 21] can now be synthesised. However, the presence of even a small fraction of linear contaminants dramatically slows their dynamics through ring-linear interpenetration [11, 22]. This slowing down shares some similarities with the one computationally discovered in systems of pure rings [23–26], where inter-ring threadings are conjectured to drive a “topological glass” state due to the emergence of a hierarchical network of threadings that serve as quasi-topological constraints [27–30]. In ring-linear blends the linear chains cannot set up a hierarchical network of constraints and the rings are thus bounded to relax on time-scales comparable to the reptative disengagement of the linear chains which perform most of the threadings; this restricts any opportunities for tuning bulk rheology via polymer design.

To overcome this limitation, and inspired by recent technical progress [31], here we investigate the behaviour of polymer architectures that simultaneously support linear and circular features. We dub these architectures “chimeric” – the name given to any mythical animal formed from parts of various other animals (Fig. 1A). The simplest example of a chimeric architecture is that of a tadpole-shaped polymer; “tadpole” for brevity (see Fig. 1B–C), which has recently been realised experimentally [31].

In this Letter, we report the first Brownian Dynam-

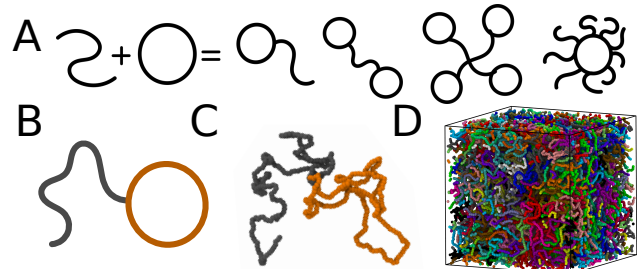


Figure 1. **A** Chimeric polymers from circular and linear chains fused together. **B** Tadpole-shaped polymers are the simplest such chimeric structure, shown as a schematic with orange “head” and grey “tail”. **C** Typical simulated conformation of a tadpole and **D** an equilibrated system of 80 tadpoles. Here the circular and linear sections both have 250 monomers, written $(C, L) = (250, 250)$.

ics simulation (Fig. 1D) of tadpole-shaped polymers in entangled solutions. We observe a dynamical transition in which systems of tadpoles with long enough tails display much slower dynamics than a corresponding system of linear chains with equal mass. We highlight that this regime cannot be readily achieved in standard blends of ring and linear chains since there is no strategy to slow down the linear fraction more than their reptative dynamics and that it is only expected to arise at asymptotically large lengths in systems of pure rings [28]. Additionally, we employ a well established algorithm based on minimal surfaces [26] to measure the statistics and correlations of inter-tadpole threadings and to explicitly connect them to the micro-rheology of the system.

Tadpole Microrheology – We model tadpole-shaped polymers as bead-spring chains made of a “tail” (linear) and a “head” (circular) components. The monomers are

connected by finitely extensible (FENE) bonds and we impose a persistence length $l_p = 5\sigma$, where σ is the typical size of a monomer, via a Kratky-Porod potential (see SM). The junction between head and tail is freely flexible and we consider athermal solvents in which the beads interact via a purely repulsive Lennard-Jones (WCA) potential [32]. The total number of monomers forming the M chains in the system is N and the overall monomer density is fixed at $\rho = NM/V = 0.1\sigma^{-3}$. With these choices, the corresponding entanglement length for a system of linear chains is $N_e = 40$. The simulations are performed at fixed volume and temperature by weakly coupling the dynamics of the monomers with a heat bath via LAMMPS [33] (see SM).

To characterise the dynamics of the tadpoles we measure the averaged mean-square displacement (MSD) of their centre of mass (CM) as $g_3(t) = \langle [\mathbf{r}_i(t_0 + t) - \mathbf{r}_i(t_0)]^2 \rangle$, where $\mathbf{r}_i(t)$ is the position of the CM of the i -th tadpole at time t and $\langle \dots \rangle$ indicates time and ensemble average. The trajectories of $g_3(t)$ are reported in Fig. 2A coloured according to tail length (blue $L = 100$, red $L = 250$ and green $L = 400$) and lighter shades of a color indicate larger head size ($C = 100, 250$ and 400). We will adopt this color scheme throughout. The trajectories display a subdiffusive regime at short-intermediate times with $g_3 \sim t^{0.4}$ and the longest chains ($L = 400, C = 400$) and ($L = 400, C = 250$) appear to be still subdiffusing at the largest lagtimes allowed by our simulations. These curves also show a behaviour that can be crudely grouped into two sets: the ones with tails $L = 100$ and the others. To better visualise this separation in dynamics we compute the diffusion coefficient of the centre of mass as $D = \lim_{t \rightarrow \infty} g_3(t)/6t$. The values of D as a function of total length ($N = L + C$) are plotted in Fig. 2B where we also show the values computed for systems of pure ring ($L = 0$) and linear ($C = 0$) chains for comparison (see SM for details).

To analyse Fig. 2, we suggest the reader first considers fixed total length N and then reads off the data along a vertical line at, say, $N = 500$. One might first notice that the dynamics of the pure ring systems is faster than any of the other and that the tadpoles with shortest tail ($L = 100, C = 400$) sit in between ring and linear behaviour. This can be naively justified by the fact that rings are generally more compact than linear chains and therefore diffuse faster; thus, converting a portion of linear chain into a ring reduces the overall polymer size and should speed up its dynamics. On the other hand, the two other tadpole designs ($L = 250, C = 250$) and ($L = 400, C = 100$) display a dynamics about 10-fold slower than linear chains of same length: this cannot be understood using the previous argument.

Fig. 2B reveals more information. First, tadpoles in the large N limit with $C \gg L$ (or $C/N \rightarrow 1$) are expected to effectively behave like rings; indeed, the systems of tadpoles with short tail size ($L = 100$, blue squares) con-

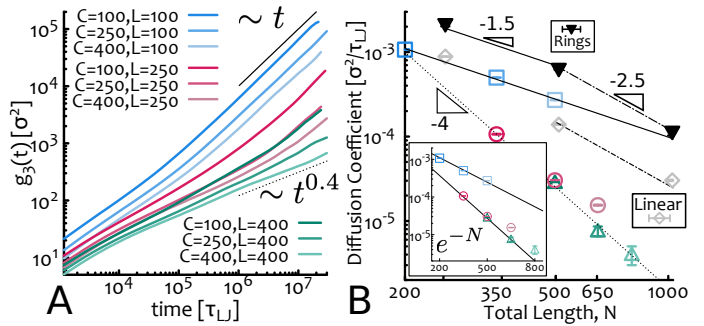


Figure 2. **A** Mean-square displacement of the centre of mass, $g_3(t)$, of the tadpoles. **B** Diffusion coefficient plotted against total contour length showing a dynamical transition between $L = 100$ for which $D \sim (C + L)^{-1.5}$ roughly compatible with that of rings (not in the asymptotic regime) and $L \geq 250$ for which $D \sim (C + L)^{-4}$ largely slower than any reptative dynamics. The values for systems of pure ring and linear chains are shown in black and grey respectively. (Inset) Shows that the decrease of D is compatible with an exponential decay. The values of D for $(C = 250, L = 400)$ and $(C = 400, L = 400)$ are upper bounds as our simulations do not reach the freely diffusive regime. The values reported for pure linear and ring polymers originate from a different set of simulations (see SM).

verge to the values of $D(L = 0, C)$ for pure rings at large N . The same is expected for the other tail sizes albeit at much larger values of N . In contrast to this, the opposite limit $C \ll L$ (or $C/N \rightarrow 0$) is not expected to lead to a system with linear-like dynamics. This is because (as we argue later on) threadings are still important even in the presence of small head and long enough tail. This effect can be appreciated as $D(L, C = 100)$ (darkest shades of blue, red and green) are slower than any of the linear systems.

The last important feature is that there is a clear dynamical transition: systems with $L = 100$ display $D \sim N^{-1.5}$ whereas ones with longer tails assume a more marked slowing down with $D \sim N^{-4}$ that is N^2 times slower than expected by reptation. [It should be noted that the decay is also compatible with $D \sim e^{-N}$, see inset of Fig. 2B]. We further note that our results are compatible with $D \sim C^{-1}L^{-3}$ (see SM, Fig. S2) as expected for the diffusion of rings in linear matrices [34, 35]. This yields $D \sim c^{-1}(1 - c)^{-3}N^{-4}$ with c the fraction of contour length in the circular head.

An important consequence of this is that by careful design of tadpole architecture one can control the dynamics over a range that is orders of magnitude broader than what can be achieved using simpler architectures within the same window of polymer length. It should also be highlighted that in ring-linear blends, the ring component is enslaved to the dynamics of the linear fraction, which cannot be slowed down further than reptation. Thus, the introduction of a substantial contamination of linear chains to enhance interpenetration does not lead to a dynamics much slower than that of a system of pure lin-

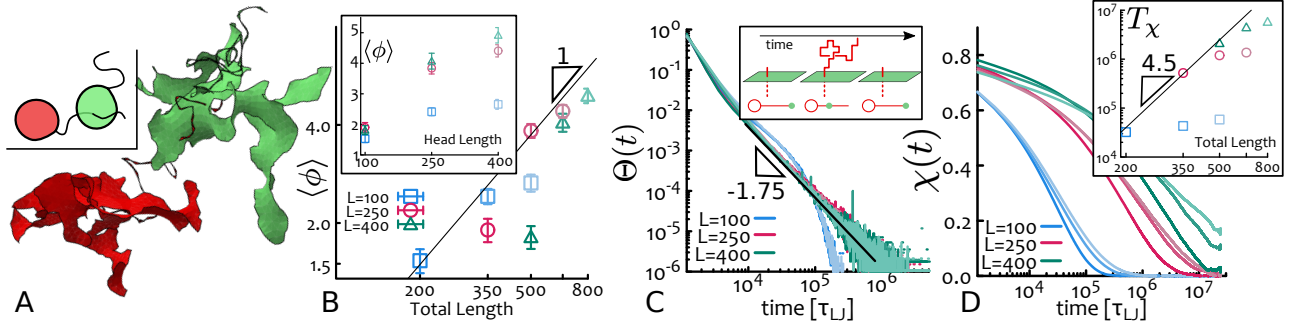


Figure 3. **A** Snapshot of two threading tadpoles with their minimal surfaces highlighted in red and green. (Inset) Sketch of the snapshot. **B** Average number of threading tails per tadpole $\langle \phi \rangle$ as a function of total chain length and (inset) head length. **C** Distribution of return times $\Theta(t)$ as defined in eq. (1) and representative fit $\sim t^{-1.75}$. (Inset) Mapping to a Brownian walk in 1D along the tail. **D** Two-point correlator $\chi(t)$. (Inset) A characteristic time T_χ plotted against N .

ear chains because the (fast) linear component becomes dominant over the (slow) circular one [11, 22]. On the contrary, with chimeric polymers, due to their fused architecture, we can set up an emergent slowing down due to collective and correlated inter-threading dynamics which we now aim to characterise.

Threadings Statistics – To characterise threadings between tadpoles we choose to employ the construction of minimal surfaces as successfully done for rings [26, 36, 37] and lasso proteins [38, 39]. The strategy is similar to the one in Ref. [26]: we first fix a boundary using the position of the beads forming the heads and realise an initial triangulated surface; we then evolve this surface via the Surface Evolver under the action of surface tension until the energy is minimised [40]. Once a minimal surface is defined per each tadpole head, we look for intersections between all possible pairs of tail and head surface (see Fig. 3A). [We choose to exclude self-intersections as it may be ill-defined in some cases]. This strategy allows us to define a time-dependent threading matrix as follows: $T_{ij}(t) = 1$ if tadpole j is threading tadpole i ($i \neq j$) and 0 otherwise. From $T_{ij}(t)$ it is natural to first extract the mean number of threadings per tadpole $\langle \phi \rangle \equiv \langle \sum_{j \neq i} T_{ij}(t) \rangle_i$, which we report in Fig. 3B: one should notice that they are abundant and in fact there can be, on average, more than one and up to five distinct chains threading any given head (often more than once).

By fixing the total length (at say $N = 500$) we observe that $\langle \phi \rangle$ is non-monotonic in tail length and that a near symmetric design is optimal for generating threadings. If tadpoles have small heads they can only accommodate a small number of threadings, yet if the head occupies a large fraction of the contour length there isn't enough mass in the tails to generate many threadings. This is confirmed by the plateauing of $\langle \phi \rangle$ for fixed tail size and increasing head length (Fig. 3B inset). Finally, it should be noted that since the head-spanning minimal surface scales linearly with head length C [26] (see SM), it is expected that also the number of threadings per head should scale linearly with C (and hence with N).

Once a tadpole is threaded by another there is a typical time during which such a threading persists and this is expected to be intimately related to its dynamics. To quantify this correlation time we compute (for each threading event) the probability of observing a threading with lifetime exactly t , i.e.

$$\Theta(t) = \langle P(T_{ij}(t) = 0 | T_{ij}(0) = 1, \dots, T_{ij}(t-1) = 1) \rangle \quad (1)$$

where $P(X | Y_1, \dots, Y_n)$ is the probability of observing X conditioned on Y_1, \dots, Y_n being observed. This calculation can be mapped to that of a first return time (or first passage time) of a Brownian Walk in 1D, whereby the walker is the intersection point moving along the tail as the threading diffuses in and out the minimal surface (as sketched in Fig. 3C). The distribution of return times of a Brownian Walk scales as $\sim t^{\alpha/2-2}$ where α is the anomalous exponent of the walk [41, 42]. In our case the tails are expected to follow a Rouse dynamics and this is confirmed by tracking the index of the bond intersecting a given minimal surface yielding a MSD with $\alpha = [0.4 - 0.6]$ (see SM). Thus, the predicted distribution of return times are expected to follow a power law with exponent $\alpha/2 - 2 = [1.7 - 1.8]$ in good agreement with our best fits to $\Theta(t)$ for $L \geq 250$ (see Fig. 3C). [The curves with $L = 100$ display a scaling exponent closer to -1.5 as their Rouse regime is shorter than our sampling time].

Importantly, the longest return time shown by $\Theta(t)$ is about 10-fold faster than the longest relaxation of the tadpoles ($10^6 \tau_{LJ}$ versus $10^7 \tau_{LJ}$). In light of this we aim to find a better quantity to relate to the tadpole dynamics. To this end we define the two-point correlator $\chi(t) = \langle T_{ij}(t) T_{ij}(t+t_0) \rangle - p_T$, where $p_T = \langle \phi \rangle / (M-1)$ is the background probability that any two tadpoles are threading at any given time. This quantity follows a stretched exponential behaviour $\chi \sim \exp\{-(t/\tau_R)^\beta\}$ with an exponent $\beta \simeq 0.3 - 0.5$ (Fig. 3D). Interestingly, the relaxation time of $\chi(t)$, i.e. the time at which $\chi \simeq 0$, is close to the crossover time to free diffusion of the tadpoles. In particular one should notice that

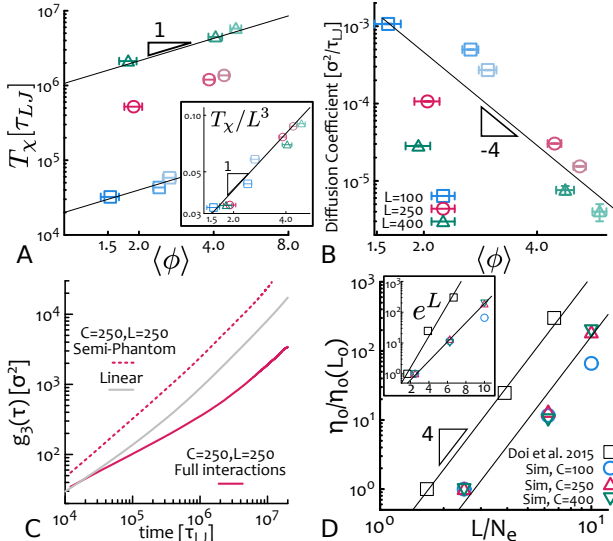


Figure 4. **A** The threading correlation time T_χ scales linearly with $\langle\phi\rangle$ with a prefactor proportional to L^3 . **B** There is a strong dependence of the diffusion constant D with the number of threadings $\langle\phi\rangle$. **C** Direct comparison of $g_3(t)$ in presence and absence of threading constraints (see text). **D** Comparison of zero-shear viscosity from simulations and experiments (Ref. [31]). The data is normalised by entanglement length and minimum η_0 in each data-set. The behaviour of η_0 against L is compatible with either a power law $\sim L^4$ or an exponential.

the two systems for which χ has not converged to zero also fail to transition to pure freely diffusive dynamics (compare with Fig. 2A). The fact that this quantity more closely recapitulate the tadpole dynamics, at least in terms of their longest relaxation time, indicates that many (un)threading events may be required before two chains become fully uncorrelated.

We can extract a characteristic time from χ as $T_\chi = \int_0^\infty \chi(t) dt$ which scales as $\sim N^{4.5}$ (Fig. 3D inset) mirroring the (inverse) behaviour of the diffusion coefficient. We also notice that $T_\chi \sim L^3 \langle\phi\rangle$ (Fig. 4A and inset) suggesting that the full relaxation of threading constraints depends on the number of threadings. This can be explained by noting that the full relaxation appears to need $\langle\phi\rangle$ serial release events before (all) the threading constraints are released.

We note that the diffusion coefficient strongly depends on the mean threading number (Fig. 4B). Exact quantification of the variation of tadpole mobility with threadings *alone* is difficult as D is also a function of total length N . In light of this, we design a symmetric (i.e. $C = 250$, $L = 250$) system of tadpoles with phantom (no steric) interactions between heads and tails, while maintaining standard self-avoidance between pairs of monomers belonging to two heads or two tails. This means that threadings of the heads by tails are no longer topological constraints for the dynamics of the tadpoles. In order to fairly compare with our other results we compress this system 2-fold (in volume) in order to maintain the effective (self-avoiding) monomer density at $\rho = 0.1\sigma^3$. We

find that the absence of effective threading results in a much faster transition to free diffusion and a 14-fold enhancement of diffusion coefficient (Fig. 4C). This finding provides independent and solid evidence that it is indeed the threadings between chains that are responsible for their correlated (subdiffusive) dynamics over long times and resulting retarded centre-of-mass diffusion. [Note that this may also be a possible explanation for a similar observation in pure ring polymers [12].]

Finally, in order to compare our results with the ones reported by Doi and co-workers in Ref. [31] we compute the zero-shear viscosity from the stress relaxation function $G(t)$, as $\eta_0 = \int_0^\infty G(t) dt$ (see SM). As shown in Fig. 4D experimental and simulated data are, first, in qualitative agreement and, second, compatible with both a power law and exponential increase as a function of tail length. Thus, within the currently computationally accessible regime, we cannot unambiguously distinguish the scaling form. Because the main mechanism of tadpole relaxation is the unthreading of tails, which is akin to arm retraction in star and branched polymers [43], we might expect exponentially long relaxation times in the long chain asymptotic regime.

Conclusions – In this work we have proposed and analysed generic systems of “chimeric” polymers formed by the combination of looped and linear topologies (Fig. 1A). The rationale for building such architectures is to achieve fine control over threading topological constraints between polymers in the system and, in turn, over the rheology of the bulk.

We discover that the dynamics of tadpole-shaped polymers is dramatically slower than that of linear counterparts of same mass provided they have long enough tails. It may be possible to leverage this phenomenology in order to design polymer architectures that can span a much larger dynamical range than that achievable with simpler architectures at fixed polymer mass. For instance, using tadpole-shaped polymers, we can explore a dynamical range that is about two orders of magnitude broader than for linear chains with modest length $N/N_e = 25$ (see Fig. 2B).

We also unambiguously demonstrate that inter-tadpole threadings play a major role in the dynamics of the tadpoles (Fig. 4C). Unexpectedly, this effect is not simply due to single threading events (Fig. 3C) but to multiple, correlated (Fig. 3D) and collective (Fig. 4A) events. Interestingly, the more the threadings per tadpole, the slower is the full relaxation of each one, thus entailing further non-linear slowing down in the large N limit (Fig. 4A) yielding a relaxation dynamics akin to that of branched or star polymers.

Finally, we argue that the phenomenology observed here might be generically expected across the broader family of chimeric polymers and that further fine tuning can likely be achieved by varying the number of looped structures, as well as their relative lengths. Our work

might therefore serve to motivate future theoretical and experimental characterisations of entangled solutions of higher-order chimeric structures which may be realised via synthetic chemistry [21] or DNA origami.

Acknowledgements – The authors would like to acknowledge the contribution and networking support by the “European Topology Interdisciplinary Action” (EU-TOPIA) CA17139. This project has also received funding from the European Union’s Horizon 2020 research and innovation programme under grant agreement No. 731019 (EUSMI). DM acknowledges the computing time provided on the supercomputer JURECA at Jülich Supercomputing Centre. JS acknowledges the support from the Austrian Science Fund (FWF) through the Lise-Meitner Fellowship No. M 2470-N28. JS is grateful for the computational time at Vienna Scientific Cluster.

* Joint first author

† davide.michieletto@ed.ac.uk

- [1] M. Doi and S. F. Edwards, *The Theory of Polymer Dynamics* (Oxford University Press, New York, 1986).
- [2] P. G. D. Gennes, *Scaling concepts in polymer physics* (1979).
- [3] J. Roovers, *Macromolecules* **21**, 1517 (1988).
- [4] D. J. Klein, *Macromolecules* **118**, 105 (1986).
- [5] M. Cates and J. Deutsch, *J. Physique* **47**, 2121 (1986).
- [6] M. Rubinstein, *Phys. Rev. Lett.* **57**, 3023 (1986).
- [7] M. Muller, J. Wittmer, and M. E. Cates, *Phys. Rev. E* **61**, 4078 (2000).
- [8] T. McLeish, *Science* (New York, N.Y.) **297**, 2005 (2002).
- [9] S. Edwards, *Proc. Phys. Soc.* **91**, 513 (1967).
- [10] F. Ferrari, *Annalen der Physik* **11**, 255 (2002).
- [11] M. Kapnistos, M. Lang, D. Vlassopoulos, W. Pyckhout-Hintzen, D. Richter, D. Cho, T. Chang, and M. Rubinstein, *Nature Materials* **7**, 997 (2008).
- [12] J. D. Halverson, W. B. Lee, G. S. Grest, A. Y. Grosberg, and K. Kremer, *J. Chem. Phys.* **134**, 204905 (2011).
- [13] T. Sakaue, *Phys. Rev. Lett.* **106**, 167802 (2011).
- [14] A. Rosa and R. Everaers, *Phys. Rev. Lett.* **112**, 118302 (2014).
- [15] D. Vlassopoulos, *Rheologica Acta* **55**, 613 (2016).
- [16] T. Ge, S. Panyukov, and M. Rubinstein, *Macromolecules* **49**, 708 (2016).
- [17] D. Michieletto, *Soft Matter* **12**, 9485 (2016).
- [18] T. Sakaue, *Soft matter* **14**, 7507 (2018).
- [19] R. D. Schram, A. Rosa, and R. Everaers, *Soft Matter* **15**, 2418 (2019).
- [20] B. W. Soh, A. R. Klotz, R. M. Robertson-Anderson, and P. S. Doyle, *Physical Review Letters* **123**, 048002 (2019).
- [21] Y. Doi, K. Matsubara, Y. Ohta, T. Nakano, D. Kawaguchi, Y. Takahashi, A. Takano, and Y. Matsushita, *Macromolecules* **48**, 3140 (2015).
- [22] J. D. Halverson, G. S. Grest, A. Y. Grosberg, and K. Kremer, *Phys. Rev. Lett.* **108**, 038301 (2012).
- [23] D. Michieletto, D. Marenduzzo, E. Orlandini, G. P. Alexander, and M. S. Turner, *Soft Matter* **10**, 5936 (2014).
- [24] E. Lee, S. Kim, and Y. Jung, *Macromol. Rapid Comm.* **36**, 1115 (2015).
- [25] D. G. Tsalikis, V. G. Mavrantzas, and D. Vlassopoulos, *ACS Macro Lett.* **5**, 755 (2016).
- [26] J. Smrek and A. Y. Grosberg, *ACS Macro Lett.* **5**, 750 (2016).
- [27] W.-C. Lo and M. S. Turner, *EPL (Europhysics Letters)* **102**, 58005 (2013).
- [28] D. Michieletto and M. S. Turner, *Proc. Natl. Acad. Sci. USA* **113**, 5195 (2016).
- [29] D. Michieletto, N. Nahali, and A. Rosa, *Phys. Rev. Lett.* **119**, 1 (2017).
- [30] D. Michieletto, D. Marenduzzo, E. Orlandini, and M. S. Turner, *Polymers* **9**, 1 (2017).
- [31] Y. Doi, A. Takano, Y. Takahashi, and Y. Matsushita, *Macromolecules* **48**, 8667 (2015).
- [32] K. Kremer and G. S. Grest, *J. Chem. Phys.* **92**, 5057 (1990).
- [33] S. Plimpton, *J. Comp. Phys.* **117**, 1 (1995).
- [34] P. J. Mills, J. W. Mayer, E. J. Kramer, G. Hadzioannou, P. Lutz, C. Strazielle, P. Rempp, and A. J. Kovacs, *Macromolecules* **20**, 513 (1987).
- [35] R. M. Robertson and D. E. Smith, *Proc. Natl. Acad. Sci. USA* **104**, 4824 (2007).
- [36] M. Lang, *Macromolecules* **46**, 1158 (2013).
- [37] J. Smrek, K. Kremer, and A. Rosa, *ACS Macro Letters* **8**, 155 (2019).
- [38] W. Niemyska, P. Dabrowski-Tumanski, M. Kadlof, E. Haglund, P. Sulkowski, and J. I. Sulkowska, *Scientific Reports* **6**, 1 (2016).
- [39] P. Dabrowski-Tumanski, W. Niemyska, P. Pasznik, and J. I. Sulkowska, *Nucleic acids research* **44**, W383 (2016).
- [40] K. A. Brakke, *Experimental Mathematics* **1**, 141 (1992).
- [41] G. M. Molchan, *Communications in Mathematical Physics* **205**, 97 (1999).
- [42] R. Metzler, G. Oshanin, S. Redner, J.-H. Jeon, A. V. Chechkin, and R. Metzler, *First-Passage Phenomena and Their Applications* **3**, 175 (2014).
- [43] T. C. McLeish, *Advances in Physics* **51**, 1379 (2002).